

Cracking Diagnosis in Fibre Reinforced Concrete Cubes and Cylinders with Synthetic Fibres using a PZT-based Health Monitoring System

Maristella E. Voutetaki¹, Maria C. Naoum², Nikos A. Papadopoulos², George Sapidis², Constantin E. Chalioris^{2*}

¹Structural Science and Technology Division, Architectural Engineering Department, School of Engineering, Democritus University of Thrace, Xanthi 67100, GREECE

²Laboratory of Reinforced Concrete and Seismic Design of Structures, Civil Engineering Department, School of Engineering, Democritus University of Thrace, Xanthi 67100, GREECE

DOI: [10.36347/sjet.2021.v09i09.004](https://doi.org/10.36347/sjet.2021.v09i09.004)

| Received: 13.09.2021 | Accepted: 18.10.2021 | Published: 22.10.2021

*Corresponding author: Constantin E. Chalioris

Abstract

Original Research Article

This paper carried out experimental research of concrete specimens with synthetic fibres under repeated splitting tension and uniaxial compression to investigate the efficiency of a proposed health monitoring methodology that implements surface-bonded piezoelectric transducers. The developed technique uses small-sized custom-made devices for diagnosing damage due to concrete cracking caused by the imposed repeated loading at various load levels. A test program of standard 150/300 mm cylinders and 150 mm cubes made of plain and fibre reinforced concrete subjected to splitting tensile and compressive repeated loading is presented and discussed. The proposed method utilises the frequency response measurements of a network of small-sized piezoelectric patches mounted to the surface of the tested specimens in order to detect the onset of damage since cracking has probably been developed in the inner concrete, whereas no visible cracks appeared on their surface. The objectives of this study also include development of a quantitative assessment procedure of damage using the statistical index values distribution at various points of measurements. The influence of distance, type of material (plain or fibrous concrete) and damage level triggers changes in the measurements of the piezoelectric transducers and the adopted statistical index seems to be a reliable assessment tool for damage quantification. Further, for the first time, a wireless and portable structural health monitoring system display feasible detection of premature cracks for damage prognosis in fibre reinforced concrete structural members.

Keywords: Fibre Reinforced Concrete (FRC); Piezoelectric lead Zirconate Titanate (PZT); Structural Health Monitoring (SHM); Damage detection; Experimental testing; Splitting tension; Compression; Repeated loading.

Copyright © 2021 The Author(s): This is an open-access article distributed under the terms of the Creative Commons Attribution 4.0 International License (CC BY-NC 4.0) which permits unrestricted use, distribution, and reproduction in any medium for non-commercial use provided the original author and source are credited.

1. INTRODUCTION

The use of fibres in concrete as mass reinforcement offers a composite material with advanced properties that drawbacks of the quasi-brittleness of plain concrete (Guerini *et al.* 2018, Marcalikova *et al.* 2020, Smarzewski 2018). Application of short discrete steel fibres have extensively been studied in concrete specimens under various loading conditions and in full-scale Reinforced Concrete (RC) structural members under monotonic (Chalioris 2013a, Gribniak *et al.* 2019, Karayannis *et al.* 2018, Kytinou *et al.* 2020a) and cyclic reversal pseudo-seismic loading (Chalioris 2013b, Chalioris *et al.* 2018, 2019, Kytinou *et al.* 2020b, Tsonos *et al.* 2021). Fibre Reinforced Concrete (FRC) is a promising alternative in civil engineering applications that received increasing attention for many years. Nowadays, the

implementation of non-metallic and sustainable materials to fibre manufacturing opens new fields of research (Smarzewski 2019).

The systematic investigation of short synthetic fibres as concrete reinforcement has recently been initiated. First studies indicated that concrete with polypropylene fibres exhibits enhanced post-cracking characteristics in terms of ductility, especially on the tensile behaviour (Bentur *et al.* 2007, Roesler *et al.* 2006, Kotecha *et al.* 2019). Synthetic fibres, as most of the used ones, arrest the opening and widening of microcracks and, therefore, FRC exhibits improved straining capacity both under tension and compression. Nevertheless, recent experimental works in this area showed that their low modulus of elasticity reduces their transference capabilities between cracks under tension stress and non-metallic fibres seem to be less

contributed to the FRC post-cracking behaviour with respect to the contribution of common steel fibres. A few studies also reported that synthetic fibres improve, rather slightly, the tensile strength in direct and indirect tests, such as splitting and bending tests (Hasan *et al.* 2011, Mobasher *et al.* 2019).

Structural Health Monitoring (SHM) in real-life RC structures is also an emerging topic of great interest. The life of RC structures can be upgraded to certain limits by SHM techniques that, eventually, could provide important information about the structural integrity and the status of these structures or of critical individual structural members (Yun *et al.* 2011). Thus, various and certain repair or/and retrofitting methods could be applied to the damaged structure timely and properly to dodge abrupt further structural degradation or even sudden collapse that could lead to severe economic losses and human casualties. A prominent solution to this issue is to perform continuous in-situ and real-time surveillance to detect perilous damages due to concrete cracking or/and steel reinforcing damages (Yang *et al.* 2008, Shanker *et al.* 2011, Talakokula *et al.* 2014, Na *et al.* 2018). Further, assessment of the severity level of the detected damages is a significant and difficult task since it employs various and complex interacting phenomena that even independently are not yet well understood.

The implementation of small-sized, surface bonded or/and embedded Piezoelectric lead Zirconate Titanate (PZT) transducers in Electro-Mechanical Admittance (EMA) based techniques has received widespread application in SHM of concrete structural members due to their favourable features (Yang *et al.* 2010, Perera *et al.* 2019, Huo *et al.* 2019). Recently, a reliable assessment method of gradually increased damages in RC structural members due to the imposed monotonic or cyclic load with increasing loading steps has been achieved using the real-time measurements of a network of PZT patches that have been installed in critical areas of the member nearby the potential damage. Applications of this SHM methodology in real-scale RC frames and beams under lateral reversal loads have been investigated by the authors (Chalioris *et al.* 2015, 2020, 2021).

Further, PZT-enabled EMA-based method has recently been addressed in concrete specimens containing short steel fibres (Wang *et al.* 2018). The effectiveness of this health monitoring technique in FRC with synthetic fibres has not been studied, to the authors' best knowledge. Furthermore, prompt diagnosis of catastrophic failures in FRC structural members due to fatigue or under seismic/ repeated loading using a real-time SHM system is a challenging task because of the vast measurements required. Research on incipient damage detection of FRC specimens is also seldom seen in literature.

This experimental study investigates the behaviour of FRC cylinders and cubes subjected to repeated splitting tension and uniaxial compression load. The efficiency of a developed SHM system that is based on PZT-enabled EMA method and uses small-sized custom-made devices for diagnosing and estimating premature damages is also examined. Quantitative assessment of the damage due to FRC cracking is also proposed using the values distribution of known statistical index results calculated by the frequency response of a network of PZT transducers mounted to the sides of the tested FRC specimens.

2. TEST PROGRAM

2.1. Materials and specimens

The concrete used in this study was a ready-mix concrete with grade C30/37 (CEN 2016) containing a commercially available ordinary Greek type cement (Portland type with pozzolan CEM II A-P 42.5 N), high fineness modulus crushed sand (fine aggregate), crushed stone aggregates with 16 mm maximum size (coarse aggregate), and water, in a mass proportion of 1:3.3:2.8:0.56, respectively. Specimens of plain concrete and FRC with synthetic fibres were casted. The length and the equivalent diameter of the used macro synthetic fibres are 50 mm and 0.715 mm, respectively, and the aspect length-to-diameter ratio equal to 70 (Figure 1a). The generic trademark of the synthetic fibres is SikaFiber Force 50. Fibres added to the fresh concrete mixture with proportion 5 kg per 1 m³ concrete. The Young's modulus under tension and the tensile strength of these fibres are 6 GPa and 430 MPa, respectively, according to manufacturer's specifications. The testing project of this study consists of six standard cylinders with dimensions 150/300 mm and six standard cubes with 150 mm size (Figure 1).

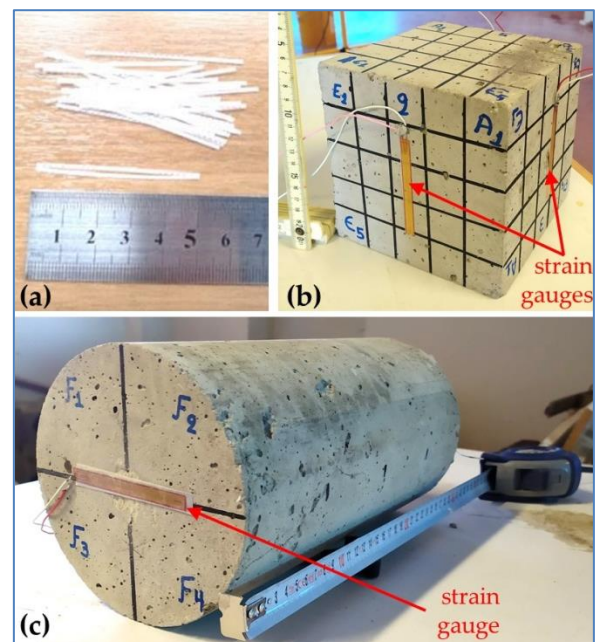


Fig-1: Specimens and fibres: (a) Macro-synthetic fibres, (b) standard cube and (c) standard cylinder with strain gauges

2.2. Test rigs and instrumentation

The entire tensile and compressive behaviour of the plain concrete and the FRC specimens are experimentally obtained by a tension/compression universal testing machine with an ultimate capacity of 3000 kN and displacement control mode. Test setups and instrumentation of both tests are illustrated in Figure 2.

Concerning the uniaxial compression tests of the cubes, three Linear Variable Differential Transducers (LVDTs) with 0.01 mm accuracy were installed to measure the compressive axial platen-to-platen deformations during testing. Further, three strain gauges mounted to the midsection of each cube's surfaces were also used to measure their axial compressive strains (see also Figure 1b). The initial elastic strains till the point of the ultimate compressive strength were recorded using the average measurements of these three strain gauges. The post-peak strain softening behaviour was recorded using the average measurements of the LVDTs since strain gauges readings were significantly disturbed due to the formation of cracks of the post-cracking response. Thus, full stress versus strain ($\sigma - \epsilon$) curves of the entire compressive behaviour can be obtained.

Concerning the splitting tension tests of the cylinders, two strain gauges mounted to the midsection of both cylinder's flat surfaces to measure the axial tensile strains (see also Figure 1c). Further, two crackmeters (displacement transducer PI) also mounted to the midsection of the flat surfaces of the cylinders to measure the opening displacement due to tensile crack propagation in plain and fibrous concrete during the post-peak tensile response (Figure 2a). Thus, initial tensile behaviour till the ultimate strength can be presented in terms of stress versus strain ($\sigma - \epsilon$) curves and the post-peak splitting tensile response can be demonstrated in terms of stress versus crack width ($\sigma - w$) curves.

2.3. Loading/displacement steps of the imposed repeated load

The cylinders were subjected to a repeated splitting tensile load (loading, unloading, re-loading,

unloading, etc.) using five (5) different load/displacement levels based on the estimated maximum splitting tensile stress. The examined load levels are denoted as follows:

1. Level “*dam1*” equals to the 20-25% of the ultimate splitting tensile strength and till this point the material has elastic properties.
2. Level “*dam2*” is a middle loading level of the ascending stress - strain part that equals to the 40-50% of the ultimate splitting tensile strength and till this point the material has, more or less, elastic properties.
3. Level “*dam3*” is at the upper ascending stress - strain part that equals to the 80-90% of the ultimate splitting tensile strength.
4. Level “*dam4*” represents a load/displacement level just right after the ultimate splitting tensile strength.
5. Level “*dam5*” is located at the softened descending $\sigma - w$ part and represents a post-peak load level that equals approximately to the 80% of the ultimate splitting tensile strength.

In similar manner, the cubes are subjected to a repeated compressive load using the following seven (7) different load/displacement levels based on the estimated maximum compressive stress:

1. Level “*dam1*” equals to the 40% of the ultimate compressive strength and till this point the material has elastic properties.
2. Level “*dam2*” level is a middle loading level of the ascending $\sigma - \epsilon$ part approximately equal to 60% of the ultimate compressive strength.
3. Level “*dam3*” level is at the upper ascending $\sigma - \epsilon$ part approximately equal to the 85% of the ultimate compressive strength.
4. Level “*dam4*” level represents a load/displacement level just right after the ultimate compressive strength.
5. Level “*dam5*” level is at the beginning of the descending $\sigma - \epsilon$ part and right after the ultimate compressive strength.
6. Level “*dam6*” level is located at the softened descending $\sigma - \epsilon$ part.
7. Level “*dam7*” represents the ultimate damage state point.

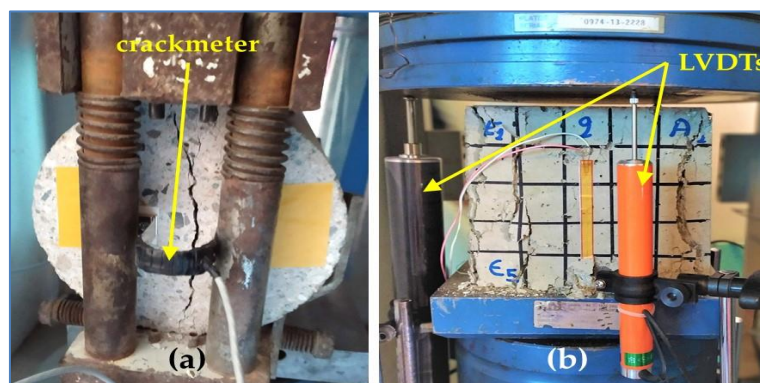


Fig-2: Test setups and typical cracking patterns: (a) Cylinder under repeated splitting tension and (b) cube under repeated uniaxial compression

3. Damage identification system and measurements

A real-time EMA and its inverse electro-mechanical impedance (EMI) methods sensing SHM system using small PZT patches is used in this study to detect and evaluate damage severity. This monitoring and damage detection SHM system first vibrates the PZT transducer, that acts as actuator, by an amplified harmonic excitation voltage. Simultaneously, it monitors the signal of the PZT, that acts now as sensor, receiving its reflected waves in terms of electrical impedance frequency response. Next, it processes the measured impedance signals in terms of voltage frequency response and, finally, it transmits the final output response to the remote user in real-time and wireless via internet connection. The full operation of this integrated SHM system can be controlled remotely from an off-site location by a terminal emulator (Providakis *et al.* 2014).

The structural impedance related to the inherent property of each PZT transducer uniquely determines the output admittance or voltage frequency response when the PZT parameters remain constant. Thus, by comparing the output signal of the SHM system at pristine (initial healthy, undamaged state) and any imminent damaged state of the host structure, any damages or anomalies occurred to the system could be identified. In concrete structural members, cracking of

the material induces change in the mechanical impedance causing a corresponding change on the voltage signal of the PZT. Additionally, the damage parameters such as the location, the direction and the width of the cracks can be determined via statistical methods.

The EMA-based SHM used in this study as a damage identification system is called “Wireless impedance/Admittance Monitoring System (WiAMS)”. It has been developed recently and tested by various experimental projects in large-scaled RC structural members by the authors (Voutetaki *et al.* 2016, Chalioris *et al.* 2015, 2020, 2021). The theoretical aspects and more details about WiAMS can be found in the aforementioned references.

The hardware of WiAMS shown in Figure 3 consists of small-sized devices that are connected to the PZT transducers (one device per each PZT patch). Each PZT patch is bonded to the concrete surface of the cylinders under repeated splitting tension by two soldered wires. Figure 3 also illustrates the exact location of six PZT transducers mounted to the surface of the cylinders; three at each side denoted as “Le1”, “Lm” and “Le2” for the left and “Re1”, “Rm” and “Re2” for the right side of the specimen.

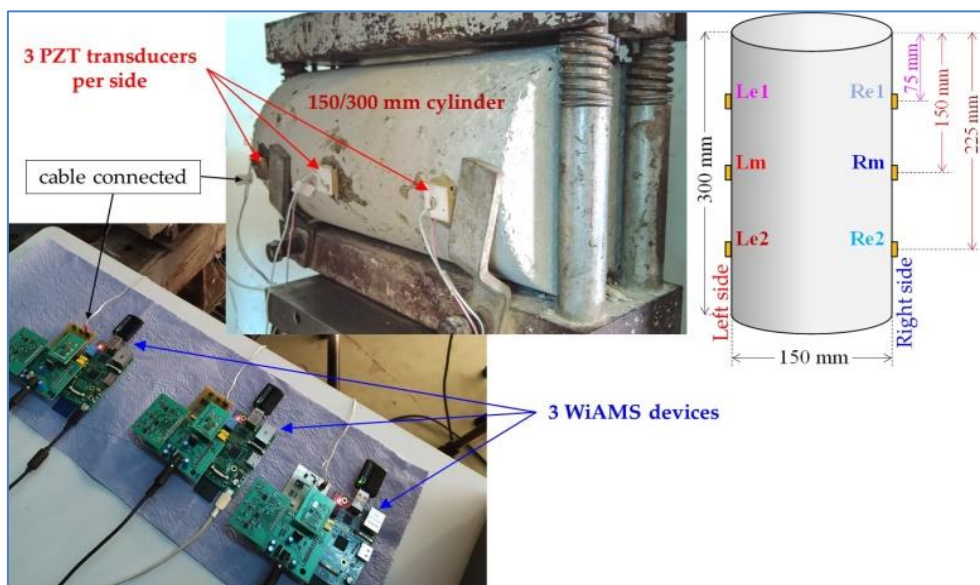


Fig-3: Devises of the developed SHM system (WiAMS) and location of the PZT patches mounted to the sides of the cylinders subjected to splitting tension test

In the case of the cubes under repeated uniaxial compression, a 30 mm width mesh has been drawn at each of the four sides of the cubes, as illustrated and numbered in Figure 4. The intersectional points of the mesh denote $4 \times 4 = 16$ specific points at each side. A PZT patch has been mounted at each point and separate measurements of the damage identification system WiAMS have been applied. This way, $16 \times 4 =$

64 measurements have been carried out at each cube specimen for each examined damage state.

In this study, WiAMS is utilized for the first time for the diagnosis and the quantitative assessment of damage at different loading/ damage levels in FRC specimens subjected to repeated splitting tensile and uniaxial compressive loading. Further, in order to quantify damage assessment in FRC, the known

statistically index of the Root Mean Square Deviation (RMSD) is employed. The signal of the PZT at the healthy state of the FRC cylinders and cubes corresponds to the baseline measurement used in the adopted statistical analysis with RMSD. Thus, variations in growth trend for the PZT output frequency response signals due to FRC cracking at different damage states could be effectively evaluated by integrating the RMSD index. Higher RMSD values indicate detection of increased structural damage.

The well-known expression for the calculation of this statistical-based index is as follows:

$$\text{RMSD} = \sqrt{\frac{\sum_1^M (|V_p(fr)|_D - |V_p(fr)|_0)^2}{\sum_1^M (|V_p(fr)|_0)^2}} \quad (1)$$

where $|V_p(fr)|_0$ is the absolute value of the voltage output signal as measured from the PZT at the “Healthy” (undamaged) state of the cube, $|V_p(fr)|_D$ is the absolute value of the corresponding voltage output signal as measured from the same PZT at the examined damage level (“dam1”, “dam2”, etc.) and M is the number of the measurements in the frequency band 10-260 kHz.

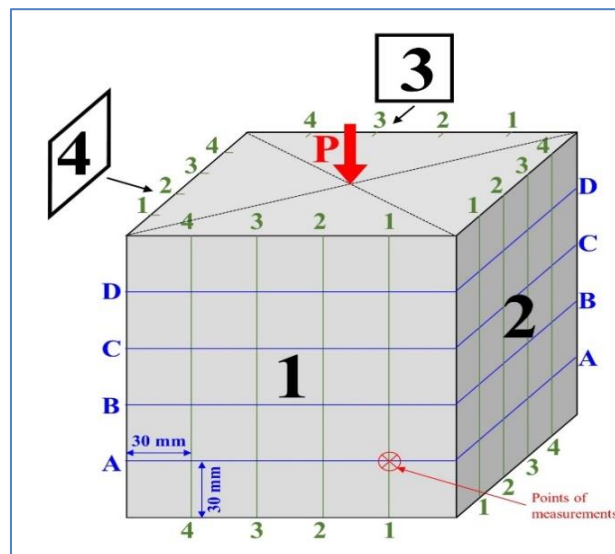


Fig-4: Notation and mesh points of measurements of the proposed cracking diagnosis procedure applied in the cubes under uniaxial compression

4. TEST RESULTS AND DISCUSSION

4.1. Splitting tensile behaviour

The experimental behaviour of typical plain concrete and FRC cylinders subjected to repeated splitting tensile loading is presented and compared in terms of stress versus strain ($\sigma - \epsilon$) and stress versus crack width ($\sigma - w$) curves in Figure 5. From these diagrams it is deduced that the splitting tensile strength of plain concrete is 2.70 MPa and equals to the tensile stress at cracking. In the case of the FRC cylinder, the splitting tensile stress at cracking is 2.83 MPa, that is only 4.8% higher than the corresponding crack stress of the plain concrete specimen. However, the comparison of the post-peak response of the specimens in terms of $\sigma - w$ reveals that the FRC cylinder exhibited 29.6%

higher maximum splitting tensile strength (3.50 MPa) than the plain concrete one. Thus, the most important influence of the synthetic fibres to the tensile behaviour is the improvement of the post-peak response since FRC cylinder displayed an important ascending part till the point of the splitting tensile strength followed by a smooth descending part with significant ductility.

It is obvious that, since plain concrete specimen did not exhibit post-cracking response, damage diagnosis measurements in this cylinder have not been performed in the post-cracking damage states “dam4” and “dam5”. The mean splitting tensile strength of the plain concrete and the FRC cylinders (six specimens from each batch) equals to 2.77 MPa and 3.51 MPa, respectively.

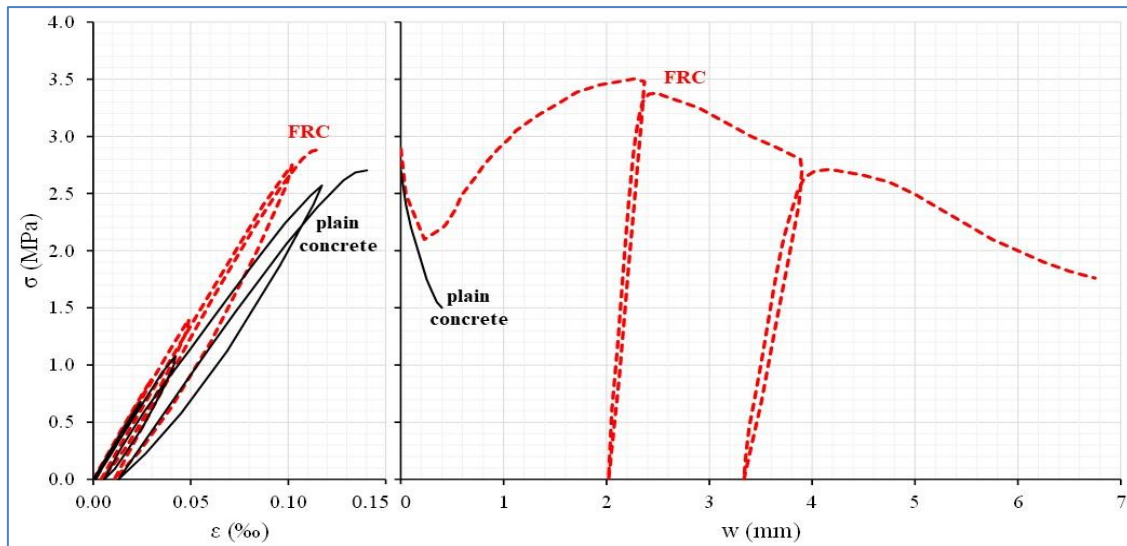


Fig-5: Stress versus strain ($\sigma - \epsilon$) and post-cracking stress versus crack width ($\sigma - w$) behavioural curves of the plain concrete and the FRC cylinders under repeated splitting tension

4.2. Uniaxial compressive behaviour

The experimental behaviour of typical plain concrete and FRC cubes subjected to repeated uniaxial compressive loading is presented and compared in terms of stress versus strain ($\sigma - \epsilon$) curves in Figure 6. From this comparison it is deduced that FRC cube exhibited 7.7% higher compressive strength (46.0 MPa) than the plain concrete one (42.7 MPa). The mean compressive strength of the plain concrete and the FRC cylinders (six specimens from each batch) equals to 42.5 MPa and 46.1 MPa, respectively.

Although FRC cube exhibited a rather slight increase, less than 10%, of the compressive strength with respect to plain concrete one, it is stressed that, the most important influence of the synthetic fibres to the compressive behaviour is the improvement of the post-peak response. The FRC cube displayed a smooth descending part in the $\sigma - \epsilon$ diagram that clearly indicates the ability of fibrous concrete to provide a rather ductile post-cracking response with respect to the brittle response of plain concrete.

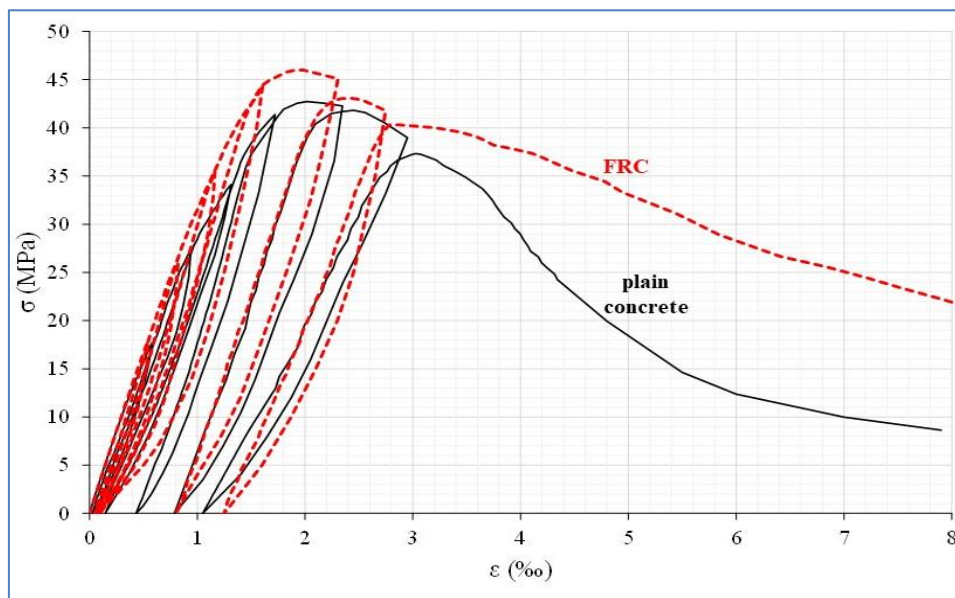


Fig-6: Stress versus strain ($\sigma - \epsilon$) behavioural curves of the plain concrete and the FRC cubes under repeated compression

4.3. Damage diagnosis and assessment

The developed SHM system has been used to diagnose damages of the plain concrete and the FRC cylinders and cubes subjected to repeated splitting tension and compression, respectively. During the splitting tensile testing procedure, measurements of the

voltage frequency responses of the six PZT transducers mounted to the cylinders have been recording at every examined loading/damage level: “Healthy” (undamaged), “dam1”, “dam2”, “dam3”, “dam4” and “dam5”.

Further, during the compressive testing procedure, measurements of the voltage frequency responses of the mounted PZT transducers have been recording at each mesh point in the cubes and at every examined loading/damage level: “Healthy” (undamaged), “dam1”, “dam2”, etc. till “dam7”. Typical diagrams of PZT responses mounted at points 1B3 and 2D1 of the FRC cube are presented in Figure 7 in terms of measured voltage versus frequency. From these diagrams it can be observed that the frequency response of PZT at point 2D1 display higher discrepancies between the pristine (“Healthy” state) and

the forthcoming damage states responses with respect to the corresponding signals of PZT at point 1B3. Further, the zoom-in views of Figure 7 diagrams reveal that as the loading/damage level gradually increases (from “dam1” that corresponds to the elastic stage till the “dam7” that represents the ultimate damage state), the corresponding frequency response curves of the damage states are more diverging from the baseline (“Healthy” curve). Thus, it is expected the RMSD values to be increase gradually along with the increase of the loading and the damage severity level of the examined specimens.

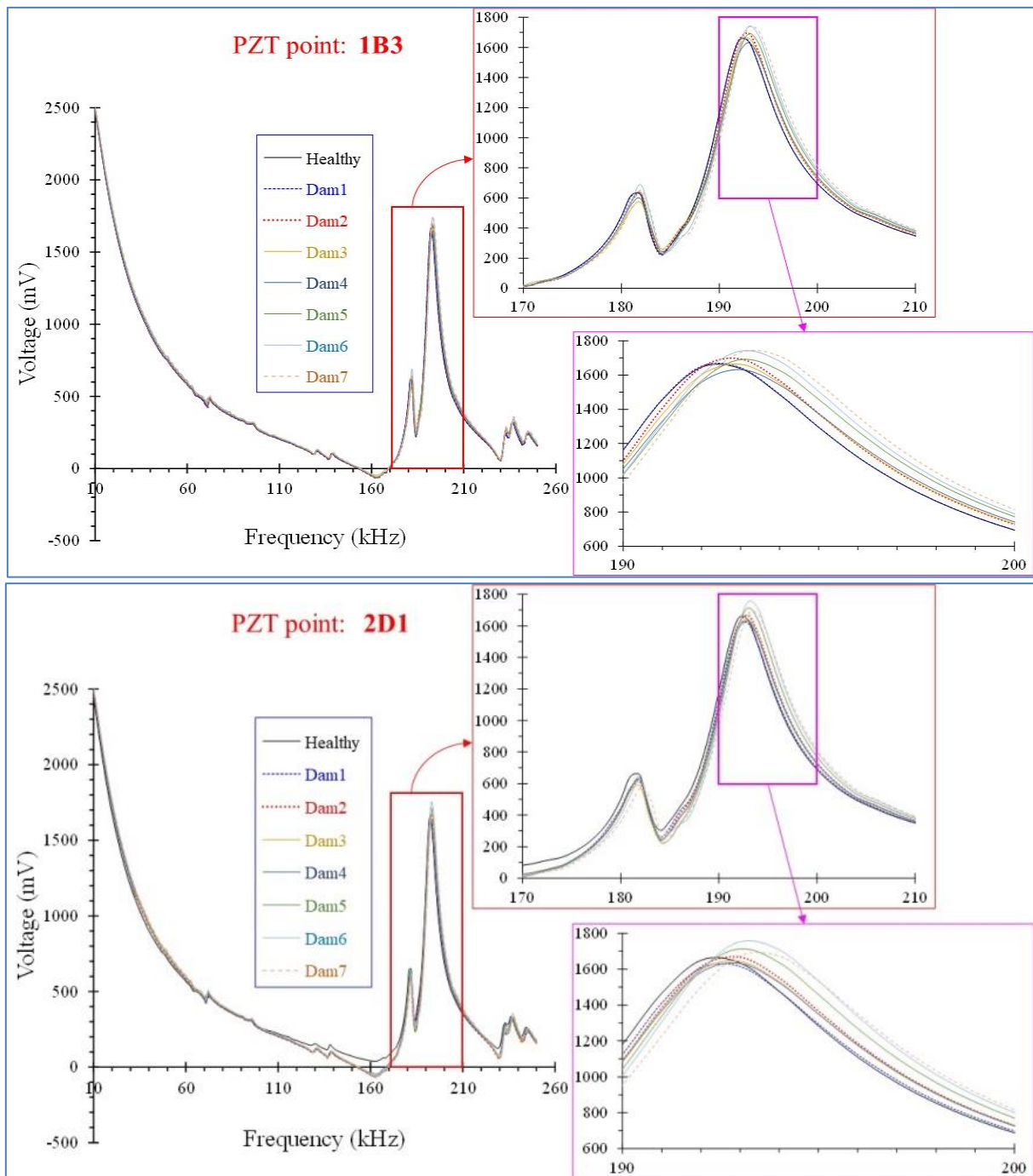
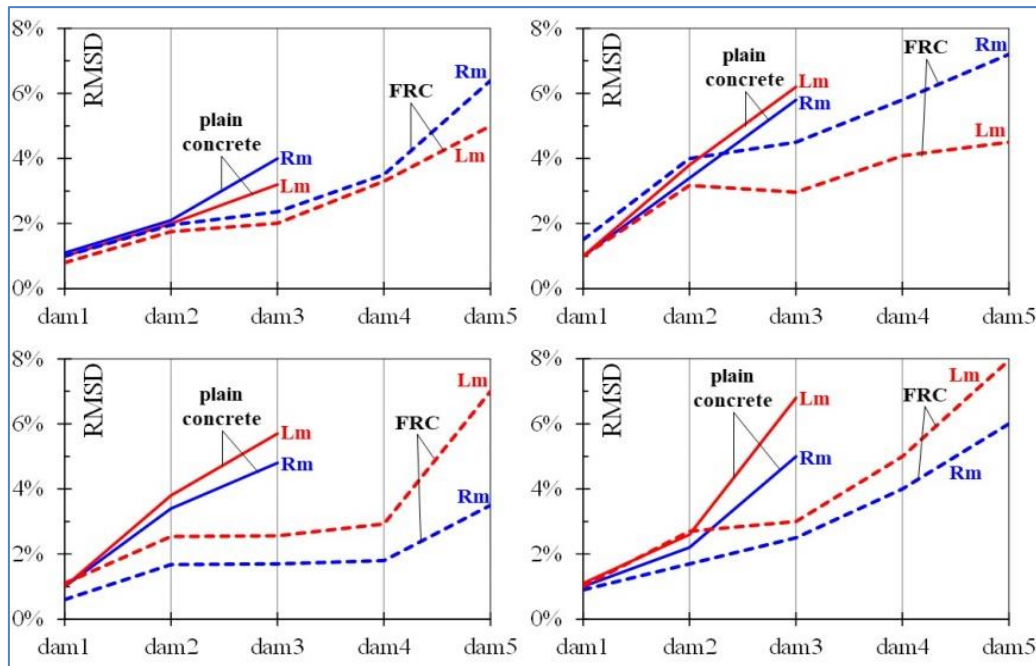


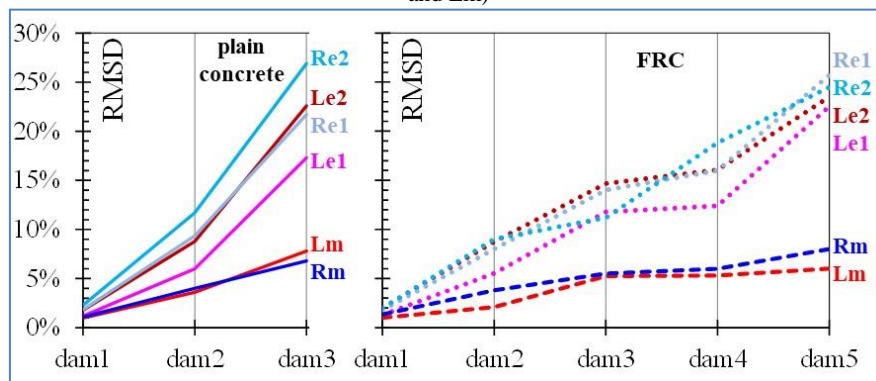
Fig-7: Typical voltage frequency response of the PZT transducers mounted to the FRC cube under repeated compression (points 1B3 and 2D1)

In order to quantify the structural damage caused by the imposed repeated splitting tensile loading, diagrams of Figure 8 illustrate the range of the RMSD values per loading/damage level that have been calculated based on the PZT voltage output signals of the plain concrete and the FRC cylinders. From these diagrams it is clearly demonstrated that higher RMSD

values indicate detection of increased structural damage. This way, the influence of damage level triggers changes in the measurements of the PZT transducers and the adopted RMSD index seems to be a reliable statistical tool for structural damage assessment in cracks due to splitting tension.



(a) Four specimens with PZT transducers located at the middle height of the cylinders and at both sides (PZT patched denoted as Rm and Lm)

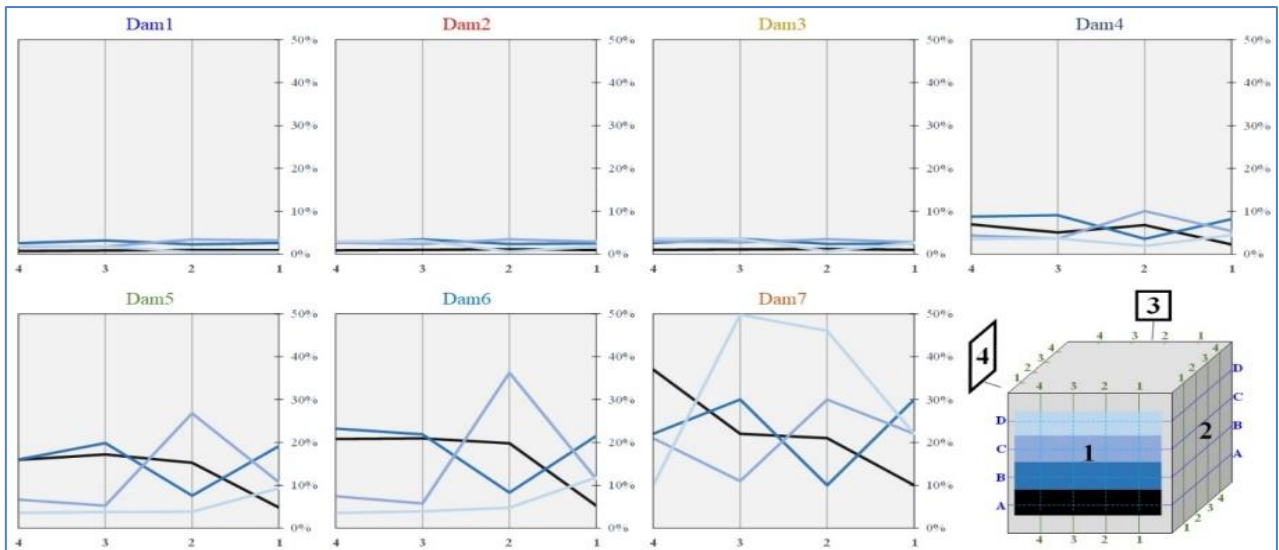


(b) Fifth specimen with all PZT transducers

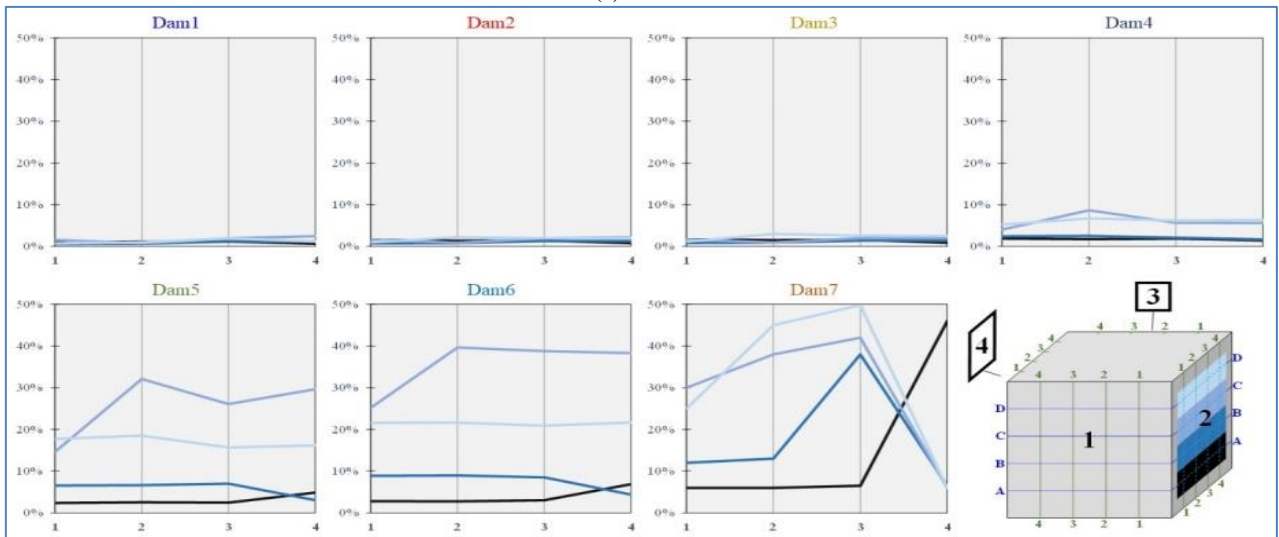
Fig-8: Damage assessment measurements in terms of RMSD index values of the plain concrete and the FRC cylinders under repeated splitting tension

Quantification of damage due to the imposed repeated compressive loading is achieved in Figures 10 and 11 that illustrate the range of the RMSD values per side of the cube that have been calculated based on the PZT voltage output signals of the plain concrete and the FRC cube, respectively. It is noted that 16-point measurements have been carried out at each side of the cube \times 4 sides \times 8 damage/loading levels = 512 total measurements at each specimen. From these graphs it can be observed that, for both plain concrete and FRC

cubes, the progressive increase of the structural damage due to the corresponding increase of the imposed compressive load can be reflected by the use of the RMSD index and the proposed SHM methodology. Further, it is deduced that RMSD values at low levels of loading such as “dam1”, “dam2” and “dam3” are very low for both specimens. This can be explained by the fact that concrete is uncracked or slightly cracked, as the $\sigma - \epsilon$ diagram of Figure 6 also indicates.

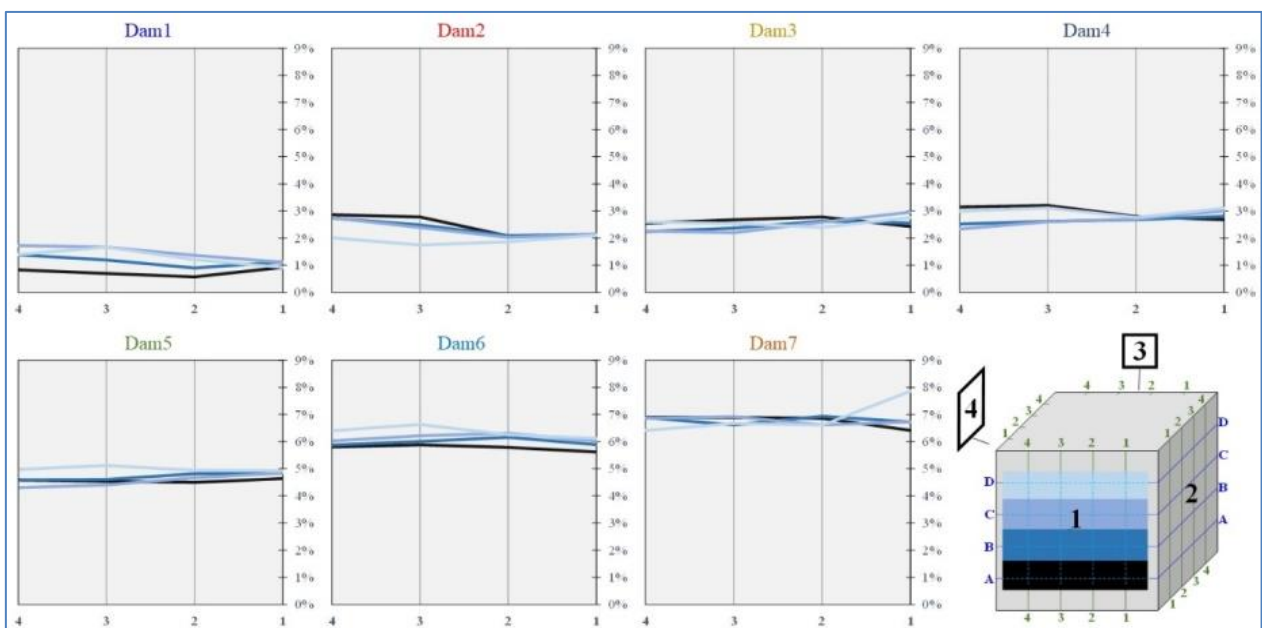


(a) Side 1

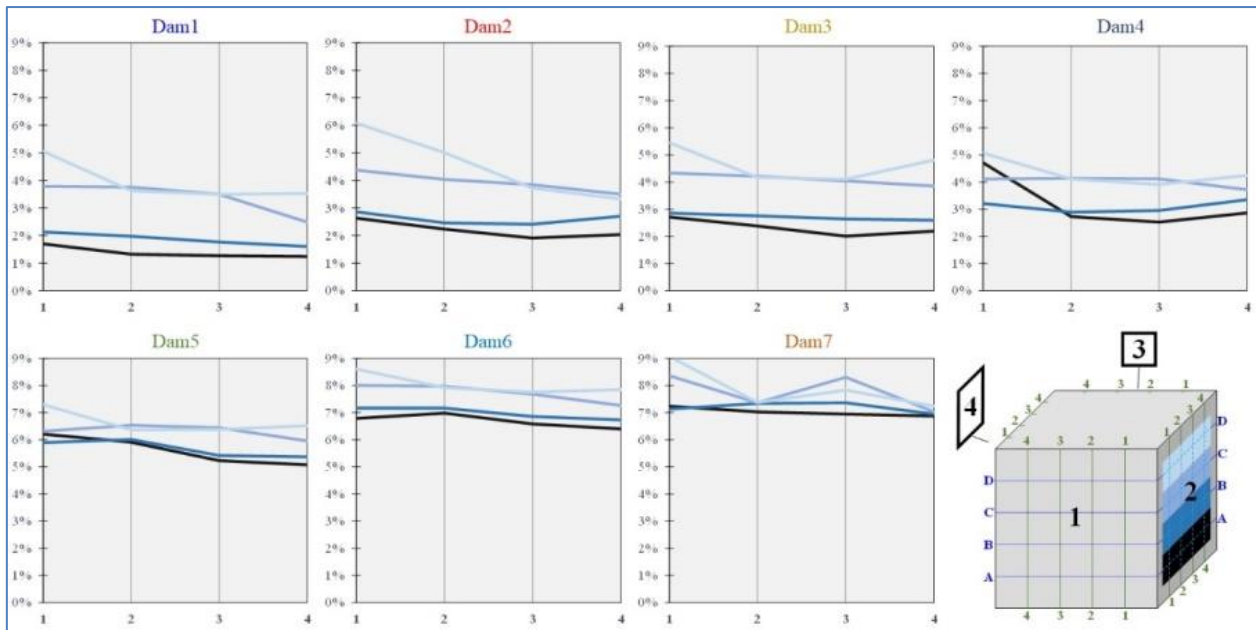


(b) Side 2

Fig-10: Damage assessment measurements in terms of RMSD index values of the plain cube under repeated compression



(a) Side 1



(b) Side 2

Fig-11: Damage assessment measurements in terms of RMSD index values of the FRC cube under repeated compression

However, after concrete cracking and especially after the maximum compressive strength, RMSD values of the plain concrete cube are significantly higher than the corresponding RMSD values of the FRC cube. This is also justified by the overall post-peak compressive behaviour of the specimens (see also Figure 6) and the existence of synthetic fibres. It is known that short fibres added in concrete as mass reinforcement mainly provide crack control due to the tensile stress transfer capability of the fibres across crack surfaces known as crack-bridging, after cracking. This way, the added synthetic fibres provide significant resistance to shear across developing cracks, and therefore, FRC cube demonstrated a pseudo-ductile response with increased residual strength and enhanced energy dissipations capacities, relative to the brittle behaviour of plain concrete. This phenomenon has been captured by the RMSD damage index with satisfactory accuracy in Figures 10 and 11.

Further, from the graphs of Figure 11 (FRC specimen) it can be observed that RMSD values have, more or less, a constant value at high loading/damage levels. This fact indicates that structural damage due to cracking in the FRC cube seems to have a uniform distribution along the entire surface of each cube side, which can be explained by the known contribution of fibres to control cracking by pre-venting opening and widening of microcracks. On the contrary, RMSD values in the plain concrete cube shown in Figure 10 display several peaks that indicate intense damage due to concrete cracking.

5. CONCLUDING REMARKS

Identification of damage due to cracking in plain concrete and FRC with synthetic fibres cylinders

under repeated splitting tension and cubes under repeated compression is achieved using a custom-made PZT-enabled EMA-based SHM system. The main contributions and conclusions of this experimental study can be summarized as follows:

- The experimental behaviour of plain concrete and FRC cylinders subjected to repeated splitting tensile loading is presented and compared in terms of stress versus strain ($\sigma - \epsilon$) and stress versus crack width ($\sigma - w$) curves. From these diagrams it is deduced that FRC cylinders exhibited 4.8% higher splitting tensile stress at cracking than the corresponding stress of the plain concrete specimen. However, the FRC cylinder exhibited 29.6% higher maximum splitting tensile strength than the plain concrete specimen that did not exhibit post-cracking response.
- The most important contribution of the synthetic fibres to the tensile behaviour is the improvement of the post-peak response since FRC cylinder displayed an important ascending part till the point of the splitting tensile strength followed by a smooth descending part with significant ductility.
- Tested FRC cubes exhibited less than 10% increase of the compressive strength with respect to plain concrete. Nevertheless, the favourable influence of the synthetic fibres is focused on the amelioration of the post-peak compressive behaviour that indicates the ability of FRC to provide increased ductility.
- The adopted SHM system and proposed damage diagnosis procedure seems efficient to identify the location and the severity level of damage.
- RMSD index values increase gradually along with the progressive increase of the imposed load and the corresponding damage severity level of the tested specimens. Especially, after concrete

cracking at post-peak compressive response RMSD values of the PC cube are significantly higher than the corresponding RMSD values of the FRC cube. This is justified by the existence of the synthetic fibres that provide a ductile post-peak behaviour with respect to the brittle response of the PC cube.

- The influence of distance, material (plain concrete or FRC) and damage level triggers changes in the measurements of the PZT transducers and the RMSD statistical index seems to be a reliable assessment tool for damage quantification.

ACKNOWLEDGEMENT

This research is co-financed by Greece and the European Union (European Social Fund - ESF) through the Operational Programme «Human Resources Development, Education and Lifelong Learning 2014-2020» in the context of the project “Structural Health Monitoring of Fi-bre-Reinforced Concrete Elements using an Advanced System of Piezoelectric Transducers” (MIS 5050596).

REFERENCES

- Bentur, A., & Mindess, S. (2007). *Fiber Reinforced Cementitious Composites: Modern Concrete Technology Series*, 2nd edition, (pp. 624). New York, USA: Taylor & Francis.
- CEN. EN 206:2013+A1:2016. *Concrete—Specification, Performance, Production and Conformity*; CEN: Brussels, Belgium, 2016.
- Chalioris, C., Providakis, C., Favvata, M., Papadopoulos, N., Angeli, G., & Karayannis, C. (2015). Experimental application of a wireless earthquake damage monitoring system (WiAMS) using PZT transducers in reinforced concrete beams. *WIT Transactions on The Built Environment*, 152, 233–243.
- Chalioris, C.E. (2013a). Analytical approach for the evaluation of minimum fibre factor required for steel fibrous concrete beams under combined shear and flexure. *Construction and Building Materials*, 43; 317–336.
- Chalioris, C.E. (2013b). Steel fibrous RC beams subjected to cyclic deformations under predominant shear. *Engineering Structures*, 49, 104–118.
- Chalioris, C.E., & Panagiotopoulos, T.A. (2018). Flexural analysis of steel fiber-reinforced concrete members. *Computers and Concrete*, 22(1), 11–25.
- Chalioris, C.E., Kosmidou, P.-M.K., & Karayannis, C.G. (2019). Cyclic response of steel fiber reinforced concrete slender beams: An experimental study. *Materials*, 12(9), 1398-1420.
- Chalioris, C.E., Kytinou, V.K., Voutetaki, M.E., & Karayannis, C.G. (2021). Flexural damage diagnosis in reinforced concrete beams using a wireless admittance monitoring system — Tests and finite element analysis. *Sensors*, 21(3), 679-704.
- Chalioris, C.E., Voutetaki, M.E., & Liolios, A.A. (2020). Structural health monitoring of seismically vulnerable RC frames under lateral cyclic loading. *Earthquakes and Structures*, 19(1), 29–44.
- Gribniak, V., Ng, P.-L., Tamulenas, V., Misiunaite, I., Norkus, A., & Šapalas, A. (2019). Strengthening of fibre reinforced concrete elements: Synergy of the fibres and external sheet. *Sustainability*, 11(16), 4456-4469.
- Guerini, V., Conforti, A., Plizzari, G.A., & Kawashima, S. (2018). Influence of steel and macro-synthetic fibers on concrete properties. *Fibers*, 6(3), 47-61.
- Hasan, M.J., Afroz, M., & Mahmud, H.M.I. (2011). An experimental investigation on mechanical behavior of macro synthetic fiber reinforced concrete. *International Journal of Civil & Environmental Engineering*, 11(3), 18–23.
- Huo, L., Cheng, H., Kong, Q., & Chen, X. (2019). Bond-slip monitoring of concrete structures using smart sensors — A review. *Sensors*, 19(5), 1231-1260.
- Karayannis, C.G., Kosmidou, P.-M.K., & Chalioris, C.E. (2018). Reinforced concrete beams with carbon-fiber-reinforced polymer bars — Experimental study. *Fibers*, 6(4), 99-119.
- Kotecha, P., & Abolmaali, A. (2019). Macro synthetic fibers as reinforcement for deep beams with discontinuity regions: Experimental investigation. *Engineering Structures*, 200, 109672-109681.
- Kytinou, V.K., Chalioris, C.E., & Karayannis, C.G. (2020a). Analysis of residual flexural stiffness of steel fiber-reinforced concrete beams with steel reinforcement. *Materials*, 13(12), 2698-2723.
- Kytinou, V.K., Chalioris, C.E., Karayannis, C.G., & Elenas, A. (2020b). Effect of steel fibers on the hysteretic performance of concrete beams with steel reinforcement — Tests and analysis. *Materials*, 13(13), 2923-2955.
- Marcalikova, Z., Cajka, R., Bilek, V., Bujdos, D., & Sucharda, O. (2020). Determination of mechanical characteristics for fiber-reinforced concrete with straight and hooked fibers. *Crystals*, 10(6), 545-566.
- Mobasher, B., Dey, V., Bauchmoyer, J., Mehre, H., & Schaef, S. (2019). Reinforcing efficiency of micro and macro continuous polypropylene fibers in cementitious composites. *Applied Science*, 9(11), 2189-2207.
- Na, W.S., & Baek, J. (2018). A review of the piezoelectric electromechanical impedance based structural health monitoring technique for engineering structures. *Sensors*, 18(5), 1307-1325.
- Perera, R., Torres, L., Ruiz, A., Barris, C., & Baena, M. (2019). An EMI-Based clustering for structural health monitoring of NSM FRP strengthening systems. *Sensors*, 19(17), 3775-3798.

- Providakis, C., Angeli, G., Favvata, M., Papadopoulos, N., Chalioris, C., & Karayannis, C. (2014). Detection of concrete reinforcement damage using piezoelectric materials — Analytical and experimental study. *International Journal of Civil, Architectural, Structural and Construction Engineering*, 8(2), 197–205.
- Roesler, J.R., Altoubat, S.A., Lange, D.A., Rieder, K.A., & Ulreich, G.R. (2006). Effect of synthetic fibers on structural behavior of concrete slabs-on-ground. *ACI Materials Journal*, 103(1), 3–10.
- Shanker, R., Bhalla, S., Gupta, A., & Kumar M.P. (2011). Dual use of PZT patches as sensors in global dynamic and local electromechanical impedance techniques for structural health monitoring. *Journal of Intelligent Material Systems and Structures*, 22(16), 1841-1856.
- Smarzewski, P. (2018). Hybrid fibres as shear reinforcement in high-performance concrete beams with and without openings. *Applied Science*, 8(11), 2070-2092.
- Smarzewski, P. (2019). Study of toughness and macro/micro-crack development of fibre-reinforced ultra-high performance concrete after exposure to elevated temperature. *Materials*, 12(8), 1210-1232.
- Talakokula, V., Bhalla, S., & Gupta, A. (2014). Corrosion assessment of reinforced concrete structures based on equivalent structural parameters using electro-mechanical impedance technique, *Journal of Intelligent Material Systems and Structures*, 25(4), 484-500.
- Tsonos, A.-D., Kalogeropoulos, G., Iakovidis, P., Bezas, M.-Z., & Koumtzis, (2021). M. Seismic performance of RC beam–column joints designed according to older and modern codes: An attempt to reduce conventional reinforcement using steel fiber reinforced concrete. *Fibers*, 9(7), 45-71.
- Voutetaki, M.E., Papadopoulos, N.A., Angeli, G.M., & Providakis, C.P. (2016). Investigation of a new experimental method for damage assessment of RC beams failing in shear using piezoelectric transducers. *Engineering Structures*, 114, 226–240.
- Wang, Z., Chen, D., Zheng, L., Huo, L., & Song, G. (2018). Influence of axial load on electromechanical impedance (EMI) of embedded piezoceramic transducers in steel fiber concrete. *Sensors*, 18(6), 1782-1799.
- Yang, Y., & Divsholi, B.S. (2010). Sub-frequency interval approach in electromechanical impedance technique for concrete structure health monitoring. *Sensors*, 10(12), 11644-11661.
- Yang, Y., Hu, Y., & Lu, Y. (2008). Sensitivity of PZT impedance sensors for damage detection of concrete structures. *Sensors*, 8, 327-346.
- Yun, C.-B., Lee, J.-J., & Koo, K.-Y. (2011). Smart structure technologies for civil infrastructures in Korea: Recent research and applications. *Structure and Infrastructure Engineering: Maintenance, Management, Life-Cycle Design and Performance*, 7(9), 673-688.